Mycobacterium tuberculosis RuvA Induces Two Distinct Types of Structural Distortions between the Homologous and Heterologous Holliday Junctions†

Jasbeer Singh Khanduja, Pankaj Tripathi, and K. Muniyappa*

Department of Biochemistry, Indian Institute of Science, Bangalore 560012, India

Received August 31, 2008; Revised Manuscript Received November 16, 2008

ABSTRACT: A central step in the process of homologous genetic recombination is the strand exchange between two homologous DNA molecules, leading to the formation of the Holliday junction intermediate. Several lines of evidence, both in vitro and in vivo, suggest a concerted role for the *Escherichia coli* RuvABC protein complex in the process of branch migration and the resolution of the Holliday junctions. A number of investigations have examined the role of RuvA protein in branch migration of the Holliday junction in conjunction with its natural cellular partner, RuvB. However, it remains unclear whether the RuvABC protein complex or its individual subunits function differently in the context of DNA repair and homologous recombination. In this study, we have specifically investigated the function of RuvA protein using Holliday junctions containing either homologous or heterologous arms. Our data show that *Mycobacterium tuberculosis ruvA* complements *E. coli* Δ*ruvA* mutants for survival to genotoxic stress caused by different DNA-damaging agents, and the purified RuvA protein binds HJ in preference to any other substrates. Strikingly, our analysis revealed two distinct types of structural distortions caused by *M. tuberculosis* RuvA between the homologous and heterologous Holliday junctions. We interpret these data as evidence that local distortion of base pairing in the arms of homologous Holliday junctions by RuvA might augment branch migration catalyzed by RuvB. The biological significance of two modes of structural distortion caused by *M. tuberculosis* RuvA and the implications for its role in DNA repair and homologous recombination are discussed.

Mycobacterium tuberculosis is an important human pathogen and a leading cause of mortality worldwide. Although much research has focused on the immunology, biochemistry, and microbiology of tubercle bacilli, knowledge about the function of a number of gene products is limited because of the lack of relevant mutants of *M. tuberculosis.* Therefore, understanding of the mechanistic basis of homologous recombination (HR)[1] may help molecular genetic analysis of mycobacteria. In this regard, isolation and characterization of *Escherichia coli* and yeast mutants have uncovered the role of HR in genetic exchange, repair of double-strand breaks, rescue of stalled replication forks, and lateral transfer. However, the mechanism of genetic exchange in mycobacteria is poorly understood. The finding that illegitimate recombination occurs at such a high frequency in *M. tuberculosis* has not been explained. Moreover, it is believed that an understanding of the biochemical roles of the enzymes and proteins of HR might provide potential novel targets for medical intervention.

Much of our understanding of the pathways and mechanistic aspects of the process of HR has emanated from studies in *E. coli* (*1*−*3*). A central step in these processes is the pairing and strand exchange between two homologous DNA molecules leading to the formation of the Holliday junction (HJ) intermediate (*1*−*4*). The branch migration and resolution of HJ intermediates in *E. coli* is promoted by RuvA, RuvB, and RuvC proteins, which participate in late stages of HR (*4*−*6*). Several lines of evidence, both in vitro and in vivo, suggest a concerted role for the RuvABC complex in the resolution of Holliday junctions (*4*−*7*). In addition to their roles during the last phase of HR, in vitro studies have demonstrated that the RuvAB complex catalyzes the regression of the replication forks (*8, 9*). Consistent with these studies, *ruvAB* was shown to be essential for the regression of the replication forks in specific replication-defective mutants (*10, 11*). However, analyses of separation-of-function *ruvA* mutants revealed that they were unable to reverse stalled replication forks but could resolve the Holliday junctions (*12*). Intriguingly, other studies have shown that *ruvAB* mutants resume DNA synthesis after UV irradiation, indicating that the RuvAB complex is not essential for DNA synthesis following the arrest at stalled replication forks (*13, 14*). However, *ruvAB* mutants, after UV irradiation, accumulate a subset of unresolved Holliday junction intermediates, leading to the loss of genome integrity (*14*).

† This research was supported by a grant from the Department of Biotechnology, New Delhi, under the "Center of Excellence" in research on mycobacteria, and a J. C. Bose National Fellowship to K.M.

* To whom correspondence should be addressed: Department of Biochemistry, Indian Institute of Science, Bangalore 560012, India. Telephone: (91-80) 2293 2235/2360 0278. Fax: (91-80) 2360 0814/0683. E-mail: kmbc@biochem.iisc.ernet.in.

[1] Abbreviations: 2-AP, 2 aminopurine; BPB, bromophenol blue; BSA, bovine serum albumin; DTT, dithiothreitol; EDTA, ethylenediaminetetraacetic acid; HJ, Holliday junction; HR, homologous recombination; IPTG, isopropyl 1-thio-β-D-galactopyranoside; MMS, methylmethane sulfonate; MtRuvA, *M. tuberculosis* RuvA protein; ODN, oligonucleotide; PAGE, polyacrylamide gel electrophoresis; SDS, sodium dodecyl sulfate.

10.1021/bi8016526 CCC: $40.75
Published on Web 12/15/2009

Structural, biochemical, and mutational analyses show that *E. coli* RuvA is a Holliday junction-specific DNA-binding protein and facilitates the interaction of RuvB with the junction (*4*−*6*). A tetramer of RuvA binds to the Holliday junction, or two RuvA tetramers sandwich the Holliday junction; on the other hand, RuvB, a member of the AAA^+ (ATPase associated with various cellular activities) family, functions as a motor protein (*15*−*20*). Together, RuvA and RuvB catalyze ATP-dependent branch migration, leading to the extension of heteroduplex DNA (*15*−*20*). The resolution of HJ is catalyzed by the RuvC endonuclease, which introduces coordinated cuts at two symmetrical sites across the junction (*21*, *22*). In vivo studies in *E. coli* have provided strong evidence that junction resolution by *ruvC* is *ruvAruvB*-dependent, and a number of biochemical and structural studies suggest the formation of a RuvABC resolvasome (*23*−*26*). Interestingly, results from crystallographic studies of *E. coli* RuvA in complex with HJ indicated that two base pairs were disrupted at the crossover point (*19*) or remained base paired (*20*). In the crystal structure of *Mycobacterium leprae* RuvA-HJ, the DNA structure was found to be disordered but the junction conformation was not described in detail (*18*).

Sequence analysis of the *M. tuberculosis* genome has revealed the presence of putative homologues of *E. coli* recombination genes, but it is unknown whether these genes can specify active proteins and whether they can carry out the catalytic reactions similar to their counterparts in *E. coli* (*27*). Moreover, in contrast to those in *E. coli*, proteins that catalyze various steps of HR in mycobacteria are ill-defined. In this regard, we previously reported that the mechanism of HR promoted by RecA and SSB from pathogenic *M. tuberculosis* differs from that of the nonpathogenic *Mycobacterium smegmatis* or *E. coli* (*28*−*31*). In fact, our current understanding of the biochemical function of *E. coli* RuvA is within the context of its interacting cellular partner, RuvB. Consequently, the inherent activities of RuvA in the contexts of DNA repair and HR are poorly understood. Currently, there are no biochemical data in terms of whether RuvA can cause base pair distortion in the arms of the Holliday junction. Exploring the functions of *M. tuberculosis* RuvA, we show that it complements *E. coli* Δ*ruvA* mutants for survival to genotoxic stress caused by different DNA-damaging agents. Purified *M. tuberculosis* RuvA binds HJ in preference to any other substrate and causes two distinct types of structural distortions between the homologous and heterologous Holliday junctions. The data presented here support models in which RuvA facilitates, in a manner independent of RuvB, base pair rearrangements in homologous and heterologous Holliday junctions.

MATERIALS AND METHODS

Bacterial Strains and Plasmids. E. coli strain Origami (DE3)pLysS and plasmid *pET21a(+)* were purchased from Novagen. *E. coli* HRS2300 is a Δ*ruvA100*::*cat* derivative of *E. coli* AB1157 (*32*) (kind gift from H. Shinagawa, Osaka University, Osaka, Japan).

Construction of the M. tuberculosis ruvA plasmid, pMTRA. The *M. tuberculosis ruvA* (Rv2593c) *ORF* sequence was obtained from www.pasteur.fr/Bio/TubercuList. The MTCY 227 cosmid, carrying the *ruv* region, was obtained from Institut Pasteur (Paris, France). The coding sequence corresponding to *ruvA* was PCR-amplified from the MTCY 227 cosmid using oligonucleotides (forward primer, 5′AAGCTGAAGGCGAATTCATGGC3′; and reverse primer, 5′GTCGGACCAAGCTTTCATCGGGCCT3′) carrying *Eco*RI and *Hin*dIII restriction sites. A single PCR cycle consisted of initial denaturation at 95 °C for 2 min followed by 30 cycles of amplification with each cycle consisting of denaturation at 95 °C for 45 s, followed by annealing at 52 °C for 45 s and extension at 72 °C for 50 s. The amplified PCR product was directionally inserted into the *pET21a(+)* expression vector, using terminal *Eco*RI and *Hin*dIII restriction sites. The resultant plasmid was designated *pMTRA*.

Purification of M. tuberculosis RuvA. RuvA protein was overexpressed in *E. coli* strain Origami (DE3)pLysS harboring the plasmid p*MTRA*. Bacteria were grown in LB broth supplemented with antibiotics (100 μg/mL ampicillin, 50 μg/mL kanamycin, and 34 μg/mL chloramphenicol) at 37 °C to OD_{600} of 0.6. RuvA was induced by the addition of 0.5 mM IPTG, and the cultures were incubated for 8 h at 37 °C. Cells were collected by centrifugation, washed in STE buffer [10 mM Tris-HCl (pH 8), 100 mM NaCl, and 1 mM EDTA], resuspended in lysis buffer [20 mM Tris-HCl (pH 8), 1 mM EDTA, 100 mM NaCl, and 10% glycerol], and stored at −80 °C. When required, cells were thawed and subjected to sonication. The sonicated suspension was centrifuged in a Beckman Ti-45 rotor at 30000 rpm for 1 h at 4 °C. Cell-free lysate was applied to a DEAE-cellulose column that had been equilibrated with TNG buffer [20 mM Tris-HCl (pH 8), 100 mM NaCl, and 10% glycerol]. RuvA was eluted in the flow-through fraction. The protein in this fraction was precipitated by the addition of solid ammonium sulfate to 80% saturation. The precipitated proteins were collected by centrifugation at 14000 rpm for 25 min at 4 °C. The pellet was dissolved in TEG buffer [20 mM Tris-HCl (pH 8), 1 mM EDTA, and 5% glycerol] containing 1 M NaCl and 5 mM 2-mercaptoethanol and dialyzed against the same buffer. The dialysate was loaded onto a Superdex-200 (HR26/60, Pharmacia) gel filtration column. Peak fractions were pooled and dialyzed against P buffer [10 mM potassium phosphate (pH 6.8), 10% glycerol, and 5 mM 2-mercaptoethanol] containing 150 mM KCl. The dialyzed fractions were applied to a hydroxyapatite Bio-Gel HTP (Bio-Rad) column which had been equilibrated with P buffer. The proteins were eluted with a 10 to 600 mM linear gradient of potassium phosphate in P buffer. Fractions containing RuvA were combined and dialyzed against TG buffer [20 mM Tris-HCl (pH 8.0), 10% glycerol, and 5 mM 2-mercaptoethanol] containing 50 mM KCl. The dialysate was loaded onto a phosphocellulose column (PII, Whatman). The bound proteins were eluted with a 50 mM to 1 M linear gradient of KCl in TG buffer. The peak fractions were combined and dialyzed against storage buffer [20 mM Tris-HCl (pH 8), 1 mM EDTA, 50 mM KCl, 50% glycerol, and 5 mM 2-mercaptoethanol]. The purity of RuvA was assessed by SDS−PAGE and found to be >98%. Aliquots of *M. tuberculosis* RuvA (MtRuvA) were stored at −80 °C.

UV Sensitivity Assay. Cultures of *E. coli* HRS2300 cells carrying vector *pET21a(+)* or *pMTRA* were grown at 37 °C for 2.5 h in LB containing 100 μg/mL ampicillin and 34 μg/mL chloramphenicol. At an OD_{600} of 0.4, the cells were collected by centrifugation and resuspended in an equal volume of M9 salts. Appropriate dilutions were made in M9

Table 1: Sequences of Oligonucleotides Used in This Study

	oligonucleotide	sequence
1	ODN1	5′GCCGTGATCACCAATGCAGATTGACGAACCTTTGCCCACGT3′
2	ODN2	5′GACGTGGGCAAAGGTTCGTCAATGGACTGACAGCTGCATGG3′
3	ODN3	5′GCCATGCAGCTGTCAGTCCATTGTCATGCTAGGCCTACTGC3′
4	ODN4	5′GGCAGTAGGCCTAGCATGACAATCTGCATTGGTGATCACGG3′
5	ODN5	5′ GCAGTAGGCCTAGCATGACAA3′
6	ODN6	5′TGACGAACCTTTGCCCACGTC3′
7	ODN7	5′ACGTGGGCAAAGGTTCGTCAATCTGCATTGGTGATCACGGC3′
8	ODN8	5′TCCGTCCTAGCAAGGGGCTGCTACCGGAAG3′
9	ODN9	5′CTTCCGGTAGCAGCCTGAGCGGTGGTTGAA3′
10	ODN10	5′TTCAACCACCGCTCAACTCAACTGCAGTCT3′
11	ODN11	5′AGACTGCAGTTGAGTCCTTGCTAGGACGGA3′
12	ODN12	5′ACGAATGTGTGTCTC[2Ap]ATCCCAACTT3′
13	ODN13	5′AAGTTGGGATTGTC[2Ap]GTGTGTAAGC3′
14	ODN14	5′TGCTTACACACTG[2Ap]GGTTAGGGTGAA3′
15	ODN15	5′TTCACCCTAACC[2Ap]GACACACATTCG3′
16	ODN16	5′GCCGTGATCACCAATGCAGATTGACGAACCTTTGCCCACGT3′
17	ODN17	5′GCCGTGATCACCAATGCAGATTGACGAACCTTTGCCCACGT3′
18	ODN18	5′GCCGTGATCACCAATGCAGATTGACGAACCTTTGCCCACGT3′
19	ODN19	5′GCCGTGATCACCAATGCAGATTGACGAACCTTTGCCCACGT3′
20	ODN20	5′GCCGTGATCACCAATGCAGATTGACGAACCTTTGCCCACGT3′
21	ODN21	5′GACGTGGGCAAAGGTTCGTCAATGGACTGACAGCTGCATGG3′
22	ODN22	5′GCCATGCAGCTGTCAGTCCATTGTCATGCTAGGCCTACTGC3′
23	ODN23	5′GGCAGTAGGCCTAGCATGACAATCTGCATTGGTGATCACGG3′
24	ODN24	5′GGCAGTAGGCCTAGCATGACAATCTGCATTGGTGATCACGG3′

salts, and cultures were UV-irradiated using an ultraviolet lamp (UVGL-58, 254 nm, G6T5 lamp). At appropriate time intervals, 100 μL aliquots were withdrawn and plated on LB agar plates supplemented with appropriate antibiotics. Colonies were counted following overnight incubation at 37 °C. For *E. coli* AB1157 and *E. coli* HRS2300 cells, the same procedure was followed except that LB medium and plates contained either no antibiotic or 34 μg/mL chloramphenicol.

MMS Sensitivity Assay. Cultures of *E. coli* HRS2300 cells carrying vector *pET21a(+)* or *pMTRA* were grown at 37 °C for 2.5 h in LB medium containing 100 μg/mL ampicillin and 34 μg/mL chloramphenicol. At an OD_{600} of 0.4, the cells were collected by centrifugation and resuspended in an equal volume of M9 salts. Appropriate dilutions were made in M9 salts, and 100 μL aliquots were plated on LB agar plates supplemented with appropriate antibiotics and the indicated concentration of MMS. Colonies were counted following overnight incubation at 37 °C. For *E. coli* AB1157 and *E. coli* HRS2300 cells, the same procedure was followed except that LB medium and plates contained either no antibiotic or 34 μg/mL chloramphenicol.

DNA Substrates. The sequences of oligonucleotides used in this study are listed in Table 1. The oligonucleotides were labeled at the 5′ end by [γ-^{32}P]ATP and T4 polynucleotide kinase (New England Biolabs) (*33*). DNA substrates were prepared by annealing the following oligonucleotides (ODNs) in the appropriate combinations: homologous Holliday junction, ODN1−ODN4; three-way junction, ODN2, ODN3, ODN5, and ODN6; 5′ Flap, ODN2, ODN3, and ODN6; Y duplex, ODN2 and ODN3; and linear duplex, ODN1 and ODN7. The heterologous HJ was prepared by annealing ODN8−ODN11. The Holliday junction with heterologous arms containing 2-aminopurine was prepared using ODN12−ODN15. Similarly, the homologous HJ containing 2-aminopurine was prepared using ODN16−ODN24. For each substrate, stoichiometric amounts of purified ODNs were annealed in 100 μL of 0.3 M sodium citrate buffer (pH 7) containing 3 M NaCl. The reaction mixtures were heated for 2 min at 95 °C followed by slow cooling to 4 °C over a period of 2 h. The annealed substrates were electrophoresed on an 8% (w/v) polyacrylamide gel in 89 mM Tris-borate buffer (pH 8.3) containing 1 mM EDTA. The bands were excised from the gel and eluted into TE buffer [10 mM Tris-HCl (pH 7.5) and 1 mM EDTA]. The identity of the DNA substrates was ascertained by restriction digestion (data not shown).

Electrophoretic Mobility Shift Assay. Reaction mixtures (20 μL) contained 50 mM Tris-HCl (pH 8), 5 mM EDTA, 1 mM DTT, 100 μg/mL BSA, the indicated ^{32}P-labeled DNA, and MtRuvA. Reaction mixtures were incubated at 4 °C for 30 min. Reaction was terminated by the addition of 2 μL of loading dye [0.1% (w/v) bromophenol blue and xylene cyanol in 20% glycerol]. The samples were electrophoresed on an 8% polyacrylamide gel in TAE buffer [6.7 mM Tris-HCl (pH 8), 3.3 mM sodium acetate, and 2 mM EDTA] at 80 V for 16 h at 4 °C. The gels were dried, and the bands were visualized using a Fuji FLA-5000 phosphorimager, followed by autoradiography. In the presence of divalent cations, EDTA was omitted, and the reaction mixtures contained either 0.5 mM $MgCl_2$ or 0.5 mM $CaCl_2$. The samples were analyzed on an 8% polyacrylamide gel in TA buffer [6.7 mM Tris-HCl (pH 8) and 3.3 mM sodium acetate containing 0.2 mM $MgCl_2$ or $CaCl_2$].

DNase I Footprinting. DNase I footprinting was performed as described previously (*34*, *35*). Reaction mixtures (20 μL) contained 100 nM ^{32}P-labeled HJ in 50 mM Tris-HCl (pH 8), 1 mM DTT, 100 μg/mL BSA, and increasing concentrations of MtRuvA. Samples were incubated for 30 min at 4 °C. Reactions were initiated by the addition of a 50 μL solution (5 mM $MgCl_2$, 5 mM $CaCl_2$, and 100 μg/mL yeast tRNA) and DNase I to a final concentration of 0.005 unit. After incubation for 1 min at 25 °C, the reactions were terminated by the addition of EDTA to a final concentration of 25 mM. DNA was precipitated with ethanol and washed with 70% ethanol, and the pellet was dried under vacuum. The pellet was resuspended in loading dye [80% (v/v) formamide, 0.1% (v/v) BPB, and 0.1% (v/v) xylene cyanol]. Maxam and Gilbert A+G ladder was prepared as described

previously (*34, 35*). DNA was heat-denatured and analyzed on a 12% polyacrylamide gel containing 7 M urea. The gel was dried, and the bands were visualized with a Fuji FLA-5000 phosphorimager, followed by autoradiography.

Chemical Probing Using Potassium Permanganate. Reaction mixtures (20 μL) contained 20 mM Tris-HCl (pH 8), 100 nM ^{32}P-labeled HJ, and increasing concentrations of MtRuvA. Samples were incubated for 30 min at 4 °C. Reaction was initiated by the addition of $KMnO_4$ to a final concentration of 1.5 mM, and the samples were further incubated for 2 min at 25 °C. In control reactions, water was substituted for $KMnO_4$. Reaction was terminated by the addition of 50 μL of stop solution [1.5 M sodium acetate (pH 5.2), 1 M 2-mercaptoethanol, and 25 μg/μL calf thymus DNA]. DNA was precipitated with ethanol and collected by centrifugation, and the pellet was dried under vacuum. The modified bases were cleaved with 1 M piperidine in a final volume of 100 μL for 30 min at 90 °C. Piperidine was removed under vacuum, and the residual pellet was washed with 100 μL of water and dried under vacuum. Maxam and Gilbert A+G ladder was prepared as described previously (*34,35*). The pellets were resuspended in formamide dye and analyzed on a 16% polyacrylamide sequencing gel containing 7 M urea. The gel was dried, and the bands were visualized with a Fuji FLA-5000 phosphorimager, followed by autoradiography.

Analysis of Global Structure by Comparative Gel Electrophoresis. Six unique junction species, each consisting of two long arms of 60 bp and two short arms of 15 bp, were prepared by hybridization of appropriate oligonucleotides as described previously (*36*). Reaction mixtures (20 μL) contained 50 mM Tris-HCl (pH 8), 1 mM DTT, 100 μg/mL BSA, 1 mM EDTA or 0.1 mM $MgCl_2$, MtRuvA (1 μM), and the indicated ^{32}P-labeled HJ substrate (2 nM). Samples were incubated for 30 min at 4 °C, loaded on a 6% polyacrylamide gel, and electrophoresed in TAE buffer [6.7 mM Tris-HCl (pH 8), 3.3 mM sodium acetate, and 1 mM EDTA] or TAM buffer [6.7 mM Tris-HCl (pH 7.5), 3.3 mM sodium acetate, and 0.1 mM $MgCl_2$]. Electrophoresis was performed at 80 V for 16 h at 4 °C. The gels were dried and the bands visualized via autoradiography.

Fluorescence Measurements. Reaction mixtures contained 20 mM Tris-HCl (pH 8), 5 mM EDTA, 1 mM DTT, the indicated HJ substrate (100 nM), and increasing concentrations of MtRuvA in a total volume of 300 μL. Steady-state fluorescence spectra were recorded on a Jobin Yvon (Horiba) Fluromax-3 fluorimeter. The fluorescence emission spectra were obtained using excitation at 315 nm. The emission spectra were recorded in the range of 330−450 nm at 10 nm intervals. The excitation and emission monochromators were set with band passes of 2 and 3 nm, respectively. The emission spectra were corrected for lamp fluctuation and instrumental variation. Tryptophan fluorescence and background emission was corrected by subtractions of control spectra, where the 2-aminopurine fluorophore was replaced with adenine. All measurements were performed at 25 °C in a 5 mm × 5 mm cuvette. The binding curves were derived from the integrated spectra from three independent measurements and normalized to the value obtained for the free junction in the absence of protein.

RESULTS

Identification and Cloning of M. tuberculosis ruvA in E. coli. To isolate the *ruvA*gene of *M. tuberculosis*, we took advantage of its published genome sequence. *M. tuberculosis ruvA* was amplified by polymerase chain reaction using appropriate forward and reverse primers corresponding to the open reading frame of *M. tuberculosis ruvA*. With these two primers, the *ruvA* gene was amplified from *M. tuberculosis* cosmid MTC Y227. PCR amplification of *M. tuberculosis ruvA* yielded a product of the predicted length (591 bp) and nucleotide sequence (data not shown). By using the terminal *Eco*RI and *Hin*dIII restriction sites (underlined in the ODN sequences) that were incorporated into the DNA during the amplification, the fragment was directionally ligated into *Eco*RI and *Hin*dIII sites of expression vector *pET21a(+)*. A clone confirmed by restriction mapping to contain a DNA fragment of the appropriate size was designated *pMTRA*. Nucleotide sequencing of the insert of *pMTRA* revealed that the fragment is the same as the reported genomic sequence of *M. tuberculosis ruvA* (data not shown). Figure 1 depicts the deduced amino acid sequence aligned with RuvA sequences from different eubacterial species and strains. Pairwise comparison of the amino acid sequence suggested that MtRuvA is 33% identical and 49% similar in sequence to *E. coli* RuvA. A similar comparison of MtRuvA with *Mycobacterium leprae* and *M. smegmatis* RuvA revealed 76 and 78% identity and 84% and 88% similarity, respectively, when compared over their entire length. On the other hand, MtRuvA is 100% identical with *Mycobacterium bovis* RuvA. There are several highly conserved regions among RuvA proteins of mycobacteria. A high degree of variability is found among the organisms in the C-terminal region (residues 140−213). However, all proposed catalytic residues in the prototype *E. coli* RuvA are conserved in MtRuvA. Since the sequence of MtRuvA is 49% similar to the *E. coli* RuvA sequence, we reasoned that the former might complement *E. coli* Δ*ruvA* mutants. This criterion assumes that *M. tuberculosis ruvA* is correctly expressed, and it makes the same interactions with *E. coli* RuvB and RuvC that its homologue makes.

UV Sensitivity of E. coli ΔruvA Mutants by M. tuberculosis ruvA. Inactivation of *ruvA* renders *E. coli* sensitive to UV radiation and genotoxic stress (*32, 37*). To complement the *E. coli* Δ*ruvA* mutation, a plasmid bearing an intact *M. tuberculosis ruvA* or the vector *pET21a(+)* was transformed into *E. coli ruvA* mutant HRS2300. The transformants were tested for their sensitivity to UV irradiation and genotoxic stress caused by methylmethane sulfonate (MMS). Complementation was assayed by plating aliquots of serial dilutions of bacteria exposed to various doses of UV radiation onto LB agar plates and subsequent incubation at 37 °C for 12 h. *E. coli* AB1157 (*ruv*$^+$) was used as a positive control. As shown in Figure 2A, small doses of UV radiation (∼50 J m^{-2}) significantly reduced the number of culturable *E. coli ruvA* mutant (HRS2300) or cells transformed with vector DNA [*pET21a(+)*]. In contrast, a UV irradiation dose of 90 J m^{-2} was required to significantly reduce the culturability of *E. coli* harboring *M. tuberculosis ruvA*, and the resistance imparted by pMTRA was comparable to that of *E. coli* AB1157 (*ruv*$^+$).

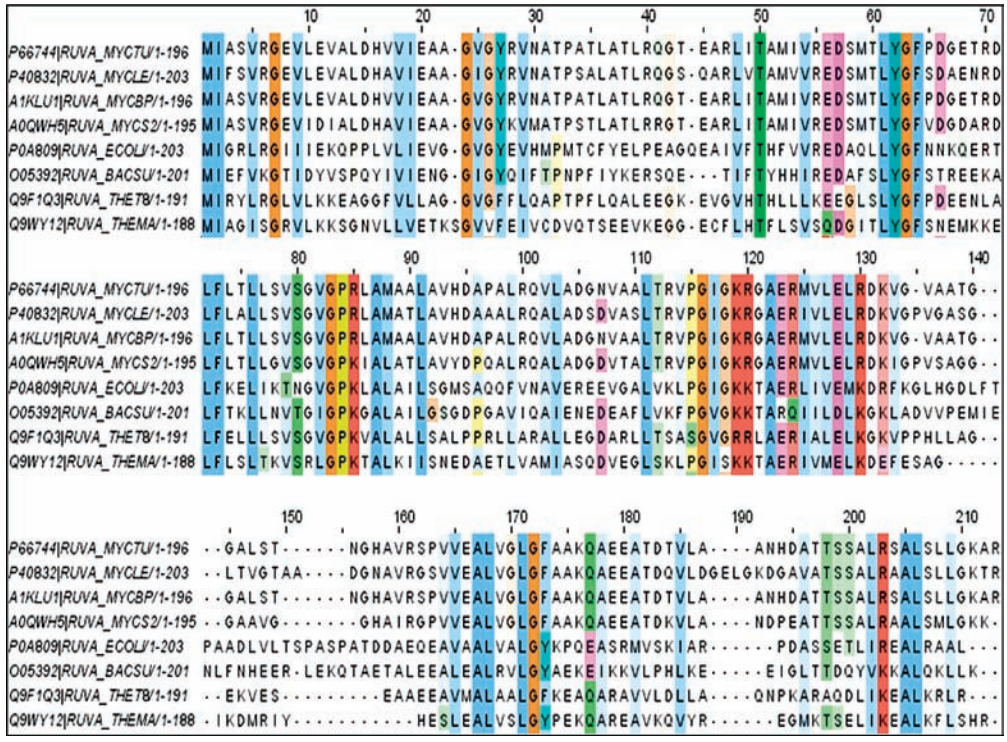

FIGURE 1: Sequence alignment of RuvA proteins from different bacterial species. Protein sequences deduced from the nucleotide sequences were aligned using the Clustal W2 program and displayed by Jalview. The conserved amino acid residues are highlighted as follows: red for hydrophobic residues, magenta for basic residues, blue for acidic residues, and green for hydroxyl/amines/glutamine. The accession numbers of the amino acid sequences used for the multiple-sequence alignment are P66744 (*M. tuberculosis* RuvA), P40832 (*M. leprae* RuvA), A1KLU1 [*M. bovis* (strain BCG/Paris 1173P2) RuvA], A0QWH5 [*M. smegmatis* (strain ATCC 700084/mc^{2}155) RuvA], P0A809 [*E. coli* (strain K12) RuvA], O05392 (*Bacillus subtilis* RuvA), Q9F1Q3 [*Thermus thermophilus* (strain HB8/ATCC 27634/DSM 579) RuvA], and Q9WY12 (*Thermotoga maritima* RuvA).

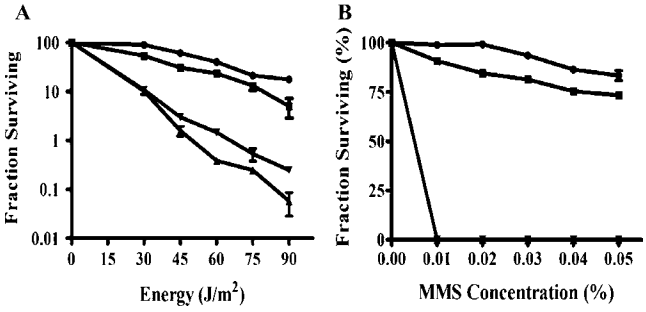

FIGURE 2: Survival of various *E. coli* strains against genotoxic stress. (A) Survival curves for UV-irradiated *E. coli* strains: (●) *E. coli* AB1157 (*ruv*$^+$), (▼) *E. coli* HRS2300 (Δ*ruvA::Cm*^{R}), (▲) *E. coli* HRS2300 [*pET21a(+)*], and (■) *E. coli* HRS2300 strain harboring the plasmid pMTRA. Each point is the average of an experiment conducted in triplicate. The error bars indicate the standard deviation. (B) Survival curves for *E. coli* strains subjected to MMS treatment: (●) *E. coli* AB1157 (*ruv*$^+$), (▼) *E. coli* HRS2300 (Δ*ruvA::Cm*^{R}), (▲) *E. coli* HRS2300 [*pET21a(+)*], and (■) *E. coli* HRS2300 strain harboring the plasmid *pMTRA*. Each point is the average of an experiment conducted in triplicate. The error bars indicate the standard deviation.

E. coli ruvA mutants display profound sensitivity to genotoxic stress (*37*). To determine whether *M. tuberculosis ruvA* (*pMTRA*) can complement the *E. coli ruvA* mutant (HRS2300), aliquots of serial dilutions of cells were plated onto LB plates containing MMS. After incubation at 37 °C for 12 h, the number of colonies appearing on the plates was counted. The strains used were the *E. coli ruvA* mutant, HRS2300, *E. coli* Δ*ruvA* (HRS2300) harboring a plasmid vector [*pET21a(+)*], or *E. coli* Δ*ruvA* (HRS2300) containing *M. tuberculosis ruvA* (pMTRA). Figure 2B shows that *E. coli ruvA* mutant (HRS2300) was killed by MMS at 0.01%, whereas the *E. coli ruvA* mutant (HRS2300) transformed with *M. tuberculosis ruvA* (*pMTRA*) exhibited resistance similar to that of *E. coli* AB1157 over the indicated concentrations of MMS, as survival in the presence and absence of MMS is comparable. These results show that *M. tuberculosis ruvA* is functional in *E. coli* and suggest that it can substitute for *E. coli* RuvA in conferring resistance to MMS and survival following UV irradiation.

Purification of M. tuberculosis RuvA. To ascertain whether *M. tuberculosis ruvA*-amplified product truly represents RuvA, we purified it for biochemical characterization. A source of large-scale preparation of RuvA was developed by allowing expression of the recombinant plasmid in *E. coli* strain Origami (DE3)pLysS. RuvA, which accumulated as a soluble protein, was detected on a SDS−polyacrylamide gel by Coomassie blue staining as a band corresponding to the deduced molecular mass (∼22 kDa). This band was absent in cell-free extracts of cultures grown in the absence of IPTG. With this heterologous expression system, RuvA accumulated to levels representing 40% of the total protein after induction with IPTG. This enabled us to monitor the progress of purification by analyzing samples at various steps by SDS−PAGE. A rapid method was developed for the purification of RuvA involving lysis of cells and chromatography on DEAE-cellulose, Superdex-200, Biogel HTP, and phosphocellulose as described in Materials and Methods. RuvA, obtained in yields of up to 3 mg/g of cell paste, was judged to be homogeneous by SDS−PAGE analysis (Figure 3). The identity of the purified MtRuvA was verified by sequencing 10 amino acid residues at the N-terminal end

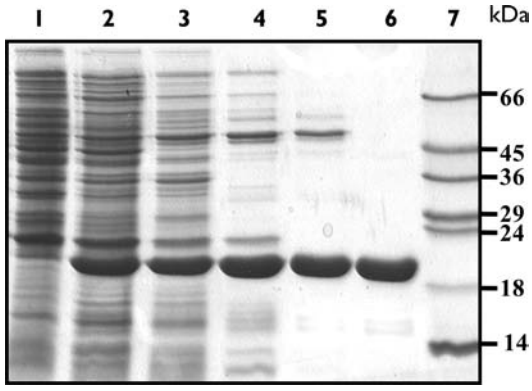

FIGURE 3: SDS−PAGE analysis showing induced expression of *M. tuberculosis* RuvA and at various stages during its purification. Twenty micrograms of proteins from the indicated sample was separated by SDS−PAGE and visualized by staining with Coomassie blue: lane 1, cell lysate from uninduced cells; lane 2, cell lysate from induced cells; lane 3, flow-through from DEAE-cellulose; lane 4, Superdex 200 gel filtration chromatography; lane 5, eluate from a hydroxyapatite column; lane 6, chromatography on a phosphocellulose column; and lane 7, standard molecular mass markers (Sigma).

and found to correspond to the *M. tuberculosis ruvA* nucleotide sequence (data not shown). Purified RuvA was devoid of ssDNA-dependent or -independent exo- or endonuclease activities (data not shown).

M. tuberculosis RuvA Binds Preferentially to the Holliday Junction. To define the biochemical functions of MtRuvA, we performed detailed investigations of DNA binding and Holliday junction processing activities of MtRuvA. The electrophoretic mobility shift assay is a simple and rapid method for studying the specificity of interaction between proteins and nucleic acids and as a means of measuring the extent of the formation of nucleic acid−protein complexes.

To examine the substrate specificity of purified MtRuvA, we constructed several intermediates involved in the pathway of recombinational DNA repair, including Holliday junctions (both branch mobile and immobile) containing 20 and 15 bp arms, respectively, a three-way junction with three 20 bp arms, a Y-shaped junction containing a 20 bp duplex arm, a flap structure containing a 20 bp duplex with a 20-nucleotide flap single strand, a duplex DNA containing hairpin structure, a 3′ single-stranded extension, a bubble structure, and a 40 bp duplex DNA, by annealing synthetic oligonucleotides (Table 1). DNA substrates were characterized as described previously (*36*, *38*). Each of these substrates, labeled at the 5′ end with [γ-^{32}P]ATP, was incubated with increasing concentrations of MtRuvA. Analysis of the reaction products by polyacrylamide gel electrophoresis, followed by autoradiography, disclosed that MtRuvA formed two distinct complexes with the mobile HJ as distinguished by differences in their relative electrophoretic mobility (Figure 4A). The relative amounts of the two MtRuvA−DNA complexes showed a strong correlation with the amount of MtRuvA added. At low concentrations (<50 nM), the predominant species was the faster-migrating complex I, whereas at higher concentrations, a slower-migrating complex II prevailed (>500 nM). The formation of nearly equimolar amounts of complex I and complex II implies the occurrence of a dynamic tetramer−octamer equilibrium model for cooperative binding of MtRuvA to the Holliday junction (Figure 4A). These results are consistent with the binding of *E. coli* (*39*) or *M. leprae* RuvA to HJ (*40*), where complex I corresponds to a tetramer (of RuvA) bound to the junction and complex II in which the junction is sandwiched between two tetramers of RuvA. Importantly, together with previous studies, these results are consistent with the notion that octamerization is a conserved property of RuvA proteins.

The formation of stable *E. coli* RuvA−HJ complexes requires divalent cations (reviewed in ref *4*). In addition, the metal ions are required for the branch migration activity of the RuvAB−protein complex. We next examined the effect of divalent metal ions on the binding of MtRuvA to the HJ. Inclusion of 0.5 mM Mg^{2+} or Ca^{2+} in reaction mixtures reduced the degree of formation of complex I, whereas their presence led to an increased level of formation of complex II (data not shown). These results indicate that binding of two tetramers of RuvA on the junction is actually favored by divalent cations. Interestingly, Ca^{2+} appeared to enhance the binding of MtRuvA to the junction, whereas complex II manifested at lower protein concentrations. The effect of cofactors on the binding of MtRuvA to HJ closely paralleled that of the prototype *E. coli* RuvA (*3*−*5*).

The efficiency of interaction of MtRuvA with the three-way junction and 5′ flap was ∼3- and 5-fold lower, respectively, compared to that of HJ. Interestingly, unlike *E. coli* RuvA, MtRuvA formed only one type of protein−DNA complex even at the highest tested concentration (Figure 4B,C). Under the conditions under which MtRuvA formed stable complexes with HJ and three-way junction, it failed to bind and form a stable complex with linear duplex DNA (Figure 4D) or with Y structure (Figure 4E). Similar results are also reported for *E. coli* RuvA (*3*−*5*). Furthermore, MtRuvA was unable to form complexes with duplex DNA containing hairpin structure, 3′ single-stranded extension, or bubble structures, indicating its high selectivity for branched DNA molecules (data not shown). These results are consistent with the architecture of the MtRuvA acidic pin (*41*), which being similar to that of *E. coli* and *M. leprae* RuvA, probably hinders its binding to linear duplex DNA (*18*, *19*). Quantification of protein−DNA complexes in the respective autoradiograms confirms robust binding of MtRuvA to HJ and substantially weaker binding affinity for the three-way junction and 5′ flap (Figure 4F). To further evaluate the relative strength of binding of MtRuvA to the HJs, RuvA−DNA complexes were titrated with increasing concentrations of NaCl. RuvA−HJ complex II was stable in the presence of 750 mM NaCl, whereas the same amount of salt induced >80% dissociation of complex I (Figure 5A,B). Taken together, these results suggest that MtRuvA interacts preferentially with Holliday junctions, compared to other intermediates of the recombinational DNA repair pathway.

M. tuberculosis RuvA Binds at the Core of the Holliday Junction. The Holliday junction resolving proteins generally bind the junction with very high affinity and specificity. This premise led us to test the junction specificity of binding of MtRuvA. To this end, we employed a mobile Holliday junction containing a very short homologous sequence at the crossover point (four nucleotide residues, which is 5′ATTG3′ in strand 1), the same substrate that had been used in gel mobility shift assays for DNA binding (see above). We assembled four identical Holliday junctions with the indicated strand labeled at the 5′ end with [γ-^{32}P]ATP. ^{32}P-labeled HJs

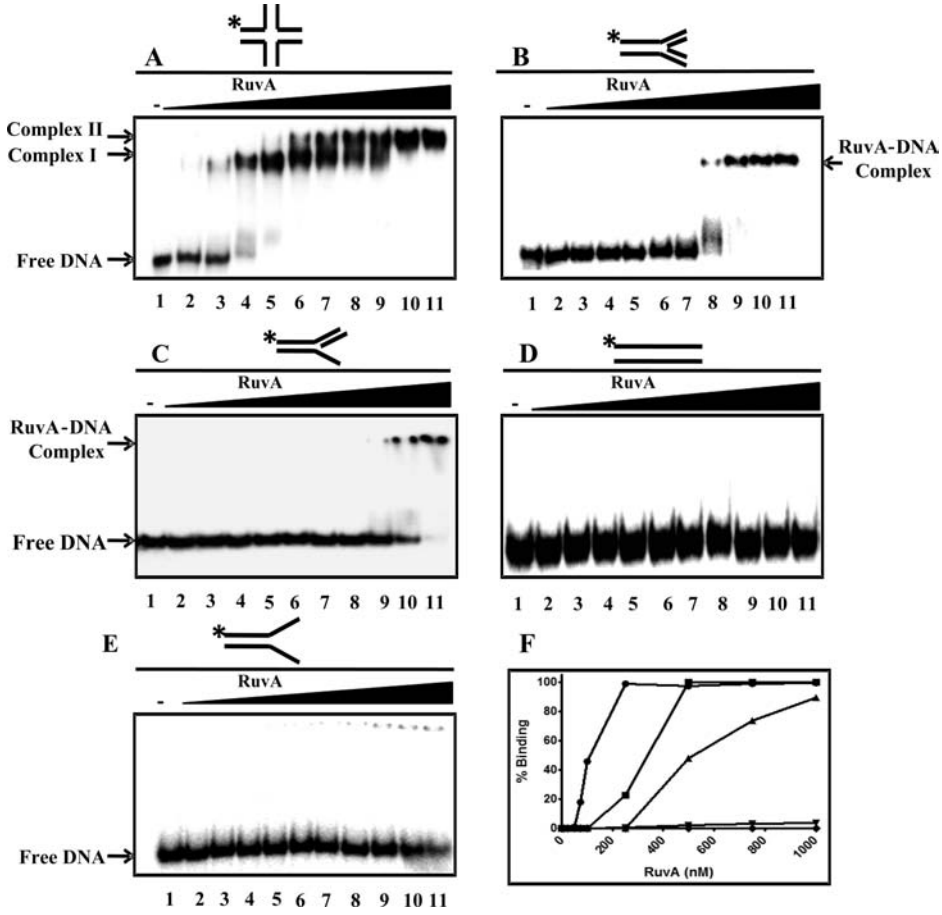

FIGURE 4: *M. tuberculosis* RuvA binds preferentially to the Holliday junction, compared to other DNA recombination intermediates. Reactions mixtures contained the indicated ^{32}P-labeled substrate (1 nM) in the absence (lane 1) or presence of 2.5, 5, 10, 25, 50, 100, 250, 500, 750, and 1000 nM MtRuvA (lanes 2−11, respectively). The filled triangle on top of the gel image denotes increasing concentrations of MtRuvA: (A) HJ containing homologous arms, (B) three-way junction, (C) 5′ flap, (D) linear duplex DNA, (E) Y junction, and (F) graphical representation of MtRuvA binding to different recombination intermediates. The extent of formation of RuvA−DNA complexes in panels A−E is plotted vs varying concentrations of MtRuvA: (●) MtRuvA−HJ complex II, (■) MtRuvA−three-way junction, (▲) MtRuvA−5′ flap DNA, (◆) MtRuvA−linear duplex DNA, and (▼) MtRuvA−Y junction. The value of each point on the curve is the average of experiments conducted in triplicate.

were incubated separately with increasing amounts of DNase I to determine its optimal concentration required to cleave the strands to the single-nucleotide level, including at the crossover point which seemingly is refractory to DNase I digestion due to steric hindrance. Subsequently, each of the HJs was incubated in the absence or presence of increasing concentrations of MtRuvA under standard conditions. The reaction mixtures were then treated with DNase I, and the products were analyzed by polyacrylamide gel electrophoresis under denaturing conditions and visualized by autoradiography. In the presence of MtRuvA, all four strands of the junction showed regions of protection, and the continuous footprint covering the area was proportional to its concentration. Interestingly, DNase I protection conferred by MtRuvA was asymmetric: the continuous footprint was 10 bp longer on one pair of symmetrical arms and 7 bp on the opposite pair of arms (Figure 6A−E). The 2-fold symmetry exhibited by MtRuvA differs from that of the prototype *E. coli* RuvA, which generated a 4-fold symmetric footprint that extends 13 bp on all the four arms (*3*, *46*). It remained possible, however, that the pattern of protection seen with the mobile junction may arise from its ability to undergo branch migration. Accordingly, we performed a DNase I footprinting assay using an immobile Holliday junction, the same HJ that had been used previously to characterize the properties of the immobile junction (*42*). The DNase I footprint generated by MtRuvA on the immobile junction revealed the extent of protection was similar to that of the mobile junction (data not shown).

Chemical Probing of the M. tuberculosis RuvA−Holliday Junction Complex. Crystallographic studies of a tetrameric form of *E. coli* RuvA bound to the Holliday junction (complex I) indicated that two base pairs were disrupted at the junction center (*19*). However, in the octameric form of the *M. leprae* RuvA−HJ complex (complex II, where two RuvA tetramers are bound to both sides of the junction), the conformational details of the junction DNA were unclear due to statistical crystallographic disorder. It has been proposed that RuvA is likely to separate the DNA strands at the crossover point, and RuvB functions as a pump to pull DNA duplex arms without segmental unwinding (reviewed in ref *5*). It is therefore important to elucidate the molecular mechanism by which RuvA, in concert with RuvB, facilitates branch migration leading to the resolution of HJ.

To explore whether RuvA binding leads to conformational changes in the HJ, we used $KMnO_4$ as a probe to detect changes in the DNA conformation of the protein-bound junction. $KMnO_4$ has been widely used for detection of distorted and single-stranded DNA regions in duplex DNA both in vitro and in vivo (*43*, *44*). We reasoned therefore

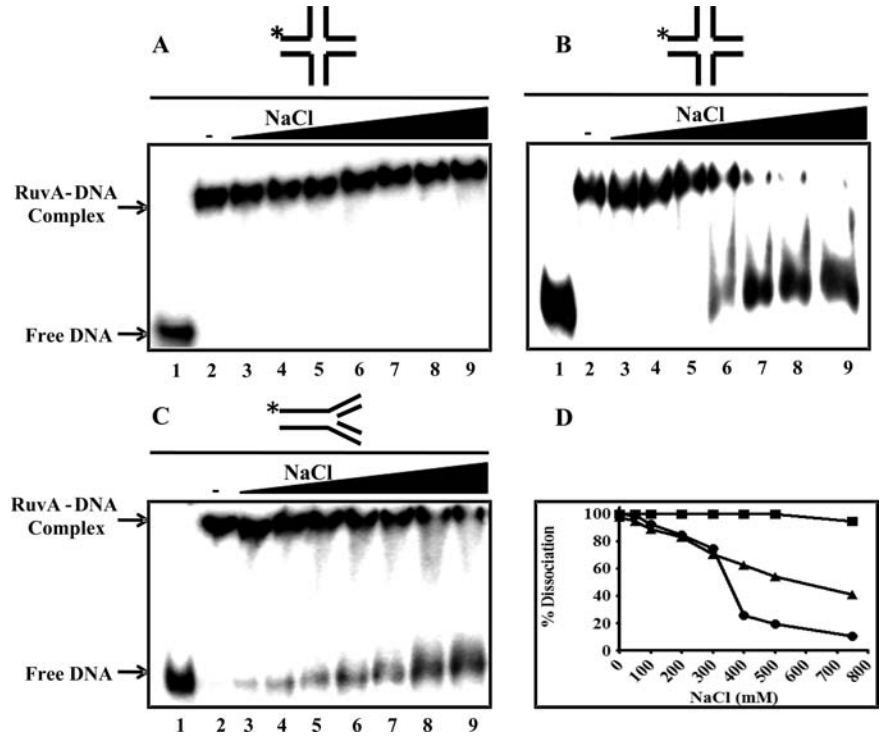

FIGURE 5: *M. tuberculosis* RuvA binds with high specificity to the Holliday junction. Reaction mixtures contained 1 nM ^{32}P-labeled HJ and MtRuvA at (A) 500 nM or (B) 50 nM or 1 nM ^{32}P-labeled three-way junction and 500 nM MtRuvA (C). After incubation for 30 min, NaCl was added to final concentrations of 50, 100, 200, 300, 400, 500, and 750 nM (lanes 3−9, respectively). After incubation for an additional 30 min, samples were electrophoresed on a polyacrylamide gel and visualized by autoradiography. (D) Graphic representation of the extent of dissociation of the MtRuvA−DNA complex containing the indicated recombination intermediate plotted vs varying concentrations of NaCl: (■) MtRuvA−HJ complex II, (●) MtRuvA− HJ complex I, and (▲) MtRuvA−three-way junction.

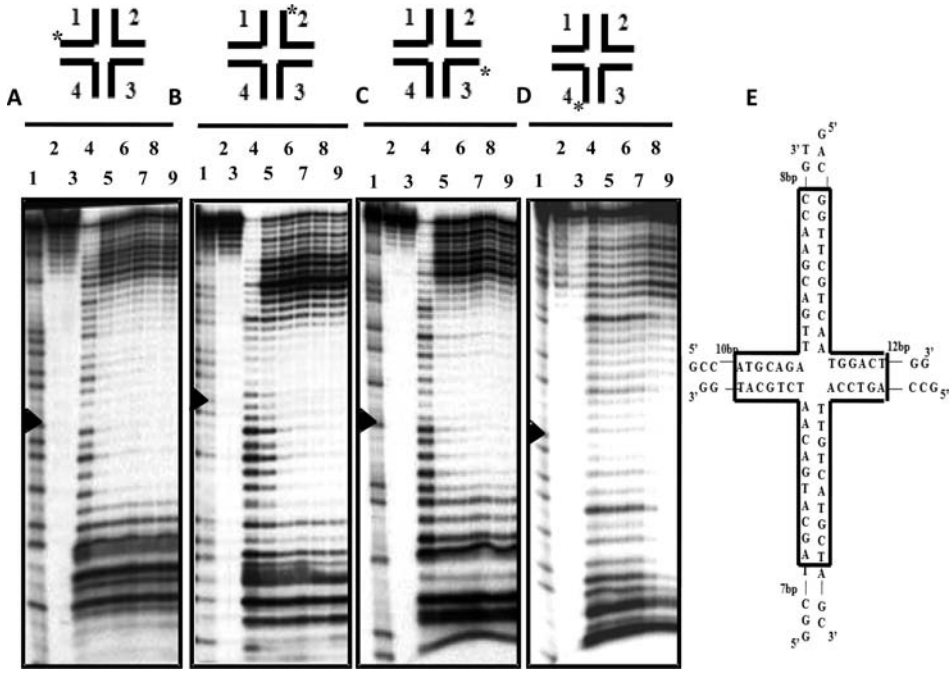

FIGURE 6: *M. tuberculosis* RuvA binds to the core of the Holliday junction. Reaction mixtures were incubated with 100 nM HJ (with 4 bp of homologous core), ^{32}P-labeled on the strand as indicated by asterisks, in the absence (lane 4) or presence of 100, 250, 500, 1000, and 2500 nM MtRuvA (lanes 5−9, respectively). Lane 1 shows a Maxam and Gilbert sequencing ladder (G+A) of the probe. Lanes 2 and 3 represents substrate and MtRuvA in the absence of DNase I, respectively. The crossover point is marked with an arrowhead on the left-hand side of each panel. The HJ diagram on the right-hand side depicts regions of protection (in the box) against DNase I digestion.

that this approach might provide insights into helical distortion of the junction following binding of MtRuvA. For this purpose, we employed the Holliday junction consisting of four immobile arms with nonhomologous sequences (*45*, *46*). In particular, we used the HJ that had been used previously to characterize the properties of the immobile junction (*42*). Each junction, which was labeled with ^{32}P on one strand at the 5′ end, was incubated with MtRuvA and then probed with $KMnO_4$ as described in Materials and Methods. As shown in Figure 7A, in the absence of MtRuvA, the T

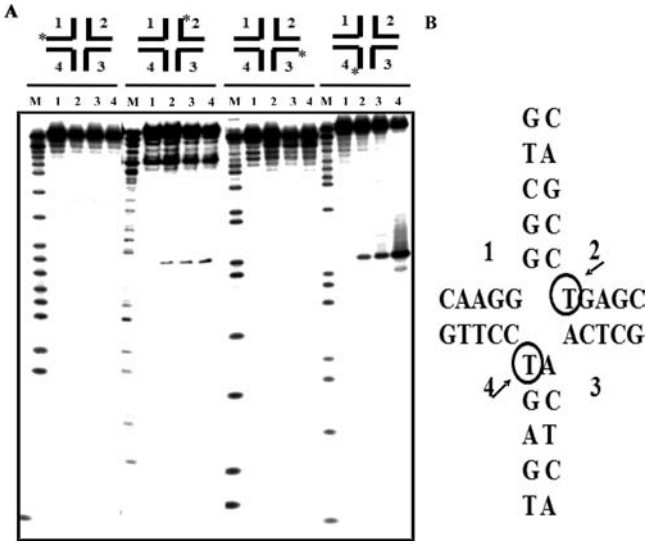

FIGURE 7: *M. tuberculosis* RuvA distorts two base pairs at the core of the nonhomologous Holliday junction. Reaction mixtures containing 100 nM HJ, labeled with ^{32}P in the specified strand by asterisk, and increasing concentrations of MtRuvA were treated with 1.5 mM $KMnO_4$. Modified T residues were cleaved with hot piperidine treatment, and products were analyzed by separation on a polyacrylamide−urea denaturing gel. (A) The first lane (M) in each panel represents the Maxam and Gilbert sequencing reaction (G+A) ladder: lane 1, HJ treated with $KMnO_4$ in the absence of MtRuvA; and lanes 2−4, HJ treated with $KMnO_4$ in the presence of 100, 500, and 1000 nM MtRuvA, respectively. (B) Hypersensitive T residues at the junction crossover are circled and denoted with arrows.

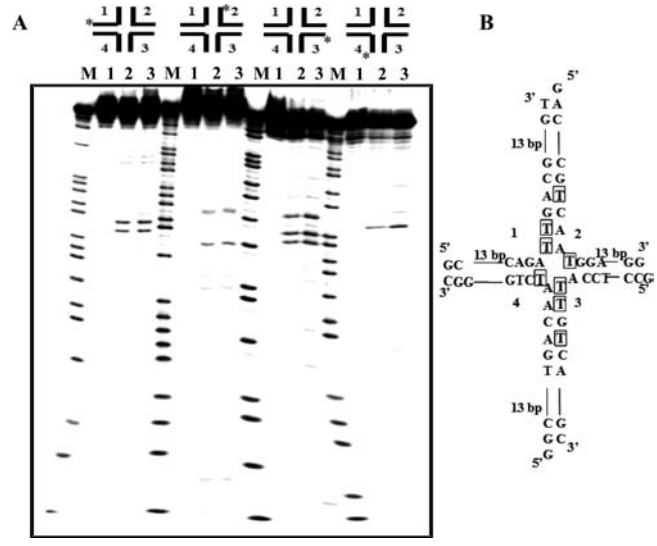

FIGURE 8: *M. tuberculosis* RuvA distorts base pairing in the arms of homologous Holliday junction. Reaction mixtures containing 100 nM ^{32}P-labeled HJ, as specified by the asterisks, and increasing concentrations of MtRuvA were treated with 1.5 mM $KMnO_4$. Modified T residues were cleaved with piperidine, and the products were analyzed on a polyacrylamide−urea denaturing gel. (A) The first lane (M) in each panel represents the Maxam and Gilbert sequencing (G+A) ladder of the probe: lane 1, HJ treated with $KMnO_4$ in the absence of MtRuvA; and lanes 2 and 3, HJ treated with $KMnO_4$ in presence of 500 and 1000 nM MtRuvA, respectively. (B) Hypersensitive T residues at the junction crossover and in the homologous core are boxed.

residues were insensitive to reaction with $KMnO_4$. In the presence of MtRuvA, the central T bases in two arms became sensitive to $KMnO_4$ and the oxidation efficiency increased with increasing protein concentrations. The position of the reactive T residues is consistent with the data from the crystal structure of the *E. coli* RuvA−HJ complex (*19*). However, the distorted region did not extend into the arms as deduced from the insensitivity of T residues to $KMnO_4$. The lack of distortion in the arms might be due to the branch-immobile core of the HJ.

The Holliday junctions generated in vivo by RecA and its eukaryotic homologues are homologous, as strand exchange between two duplex DNA molecules produces the four-way junction. However, heterologous Holliday junctions may be found in the cell during the repair of damaged DNA. Indeed, genetic evidence implicates *ruvA* and *ruvB* in DNA repair and in the processing of DNA structures, including the disrupted replication forks that arise during the normal replication (*47*). The HJ that we have employed for DNA binding studies is a mobile Holliday junction containing a very short homologous sequence at the core (four nucleotide residues), and the arms contain heterologous sequences, which stabilize the structure from spontaneous branch migration and render it amenable to experimentation. To corroborate the ability of MtRuvA to catalyze base pair rearrangements in the homologous Holliday junction, we incubated each HJ, labeled with ^{32}P on one strand at the 5′ end, in the absence or presence of increasing concentrations of MtRuvA and then probed the HJ with $KMnO_4$. Control experiments showed that the T residues were insensitive to reaction with $KMnO_4$. However, in the presence of MtRuvA, all the T residues within the homologous core were rendered sensitive to the $KMnO_4$ oxidation (Figure 8A). Figure 8B shows the residues, in square box, that were rendered sensitive to oxidation by $KMnO_4$. These results indicate that MtRuvA can independently catalyze branch migration of homologous Holliday junctions. The process of branch migration, however, is restricted to the homologous core of the junction.

M. tuberculosis RuvA Induces Two Distinct Modes of Base Pair Distortions in the Holliday Junction: Homologous versus Heterologous Cores. To independently ascertain helical distortions associated with the interaction of MtRuvA with the Holliday junctions, we substituted 2-aminopurine (2-AP) for adenine at several individual positions in all four strands of the junction. 2-AP is a sensitive fluorescent probe, whose fluorescence is quenched in the duplex DNA and enhanced when the base pair is distorted (*36*). Therefore, 2-AP has been extensively used to examine changes in the DNA structure consequent to the interaction of a variety of nucleic acid-binding proteins (*3*). We constructed a series of HJ substrates containing 2-AP to follow structural distortions upon interaction of MtRuvA. We first performed experiments with the heterologous HJ substrate, which had been previously used for cocrystallization with *E. coli* RuvA (*19*). Each HJ substrate contained a single 2-AP substitution, which is highlighted with squares (Figure 9, center panel). Panels A−D depict the fluorescence emission spectra of each Holliday junction in the absence or presence of increasing concentrations of MtRuvA (0.5−5 μM). The Holliday junctions bearing 2-AP at the core exhibited increased fluorescence with increasing concentrations of MtRuvA. The increase in fluorescence reached a maximum of 3-fold and then plateaued. On the other hand, the HJ substrates containing 2-AP one or two base pairs away from the core

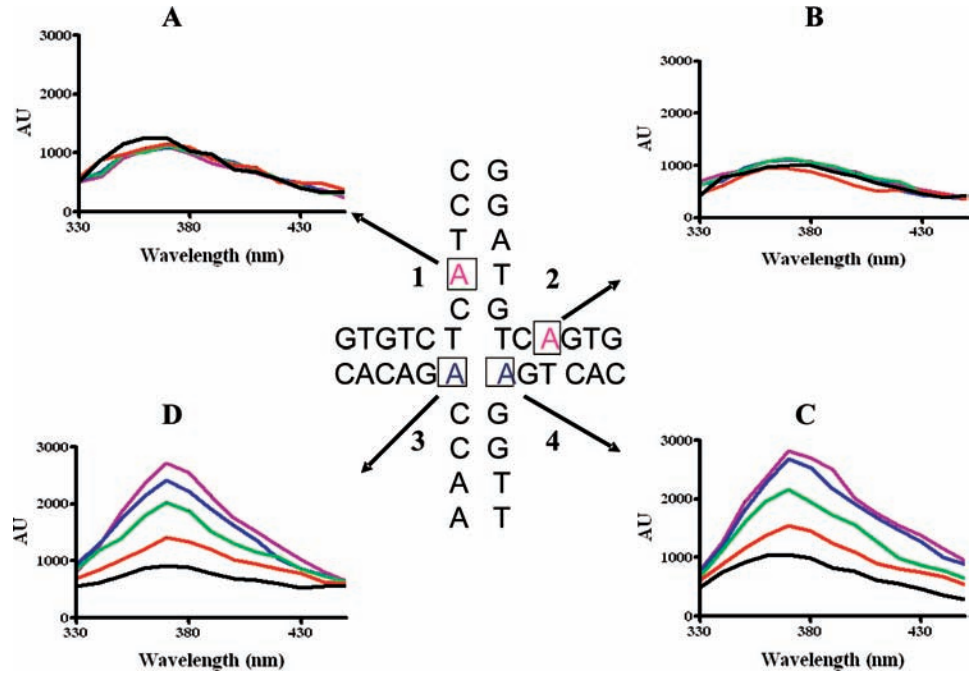

FIGURE 9: *M. tuberculosis* RuvA-induced structural distortion of nonhomologous HJ as monitored using 2-AP fluorescence. The center panel shows the positions of the adenine bases (boxed), individually substituted with 2-AP, at the junction center and in the arms of the HJ. The corrected fluorescence emission spectra were recorded, in the wavelength region between 330 and 450 nm, as a function of increasing concentration of MtRuvA. In each reaction, 100 nM junction DNA was used. (A−D) Plots of the change in fluorescence intensity (in arbitrary units), on the *Y*-axis, in the absence (black lines) or presence of MtRuvA at 0.5 μM (red lines), 1 μM (green lines), 2.5 μM (blue lines), or 5 μM (purple lines). The fluorescence emission spectrum of each HJ variant is pointed with a black arrow to its corresponding 2-AP residue in the HJ diagram depicted at the center.

displayed no measurable increase in fluorescence in the presence of increasing concentrations of MtRuvA. Taken together, these results suggest that MtRuvA causes distortion of a single base pair in the heterologous HJ at the crossover point, consistent with $KMnO_4$ footprinting data (Figure 7).

The absence of base pair distortion inside the arms of the heterologous HJ prompted us to ask whether MtRuvA induces base pair distortions in the arms of the homologous Holliday junction. To this end, we used a set of HJ substrates with arms of equal length (20 bp) and a homologous core, which can branch migrate over the central 4 bp region (i.e., 5′ATTG3′ in strand 1). 2-AP was uniquely positioned in each strand of the HJ, either at the center, adjacent to the center, or away from the center (Figure 10, square boxes in the center panel). We performed fluorescence measurements using a fixed amount of HJ substrate and increasing concentrations of MtRuvA. We observed an increase in fluorescence with HJ substrates that contained 2-AP at the center with increasing concentrations of MtRuvA (Figure 10A,E). Somewhat surprisingly, we observed increased fluorescence with those HJ substrates that contained 2-AP within a 4 bp region from the center (Figure 10 C,H). In one pair of symmetrically related arms, fluorescence enhancement reached a maximum of 3-fold and then plateaued. In contrast, in the second pair of symmetrically related arms, in which 2-AP was embedded 2−3 bp from the center, no measurable change in fluorescence was observed (Figure 10D,I). Together, these results suggest that MtRuvA causes two distinct types of base pair distortions between homologous and heterologous HJ substrates.

M. tuberculosis RuvA Changes the Global Conformation of the Holliday Junction. Previous studies have shown that *E. coli* RuvA binds the HJ as a tetramer (*39*, *48*) or double tetramer (*49*) with high affinity and unfolds the compact stacked X structure into a square-planar conformation that can branch migrate very rapidly (*50*). In addition, data from different junction processing enzymes suggest a unified concept of change in the conformation of the junction upon binding by the proteins. In particular, studies on different junction resolving enzymes have revealed changes in the overall structure and distortion of the junction DNA upon binding of junction resolvases (*36*, *51*, *52*). To explore the relationship between binding of MtRuvA and alterations in global structure and distortion of the junction DNA, we employed the established technique of comparative gel electrophoresis (*53*, *54*). To this end, we incubated a set of HJs containing two long (60 bp) and two short (15 bp) arms in the presence of either EDTA or Mg^{2+} (*36*). The six long−short arm junction species were incubated, separately, with MtRuvA under conditions that favor the formation of physiologically important complex II (see Figure 11A). MtRuvA−HJ complexes were resolved via native PAGE in parallel with a set of junctions that were not incubated with the protein.

In the presence of EDTA, the free junctions exhibited the characteristic slow−fast−slow−slow−fast−slow mobility variations, which are ascribed to the unstacked X structure in which the arms of the junction are directed toward the corner of the square (Figure 11A, lanes 1−6). However, in the presence of MtRuvA, four of the six species exhibited slow migration with long arms subtending 90°, whereas two species exhibited faster migration where the long arms are colinear (Figure 11A, lanes 7−12). In parallel, the free junctions were electrophoresed in the presence of Mg^{2+}. The HJ substrates exhibited slow−intermediate−fast−fast−intermediate−slow mobility characteristic of stacked X structure

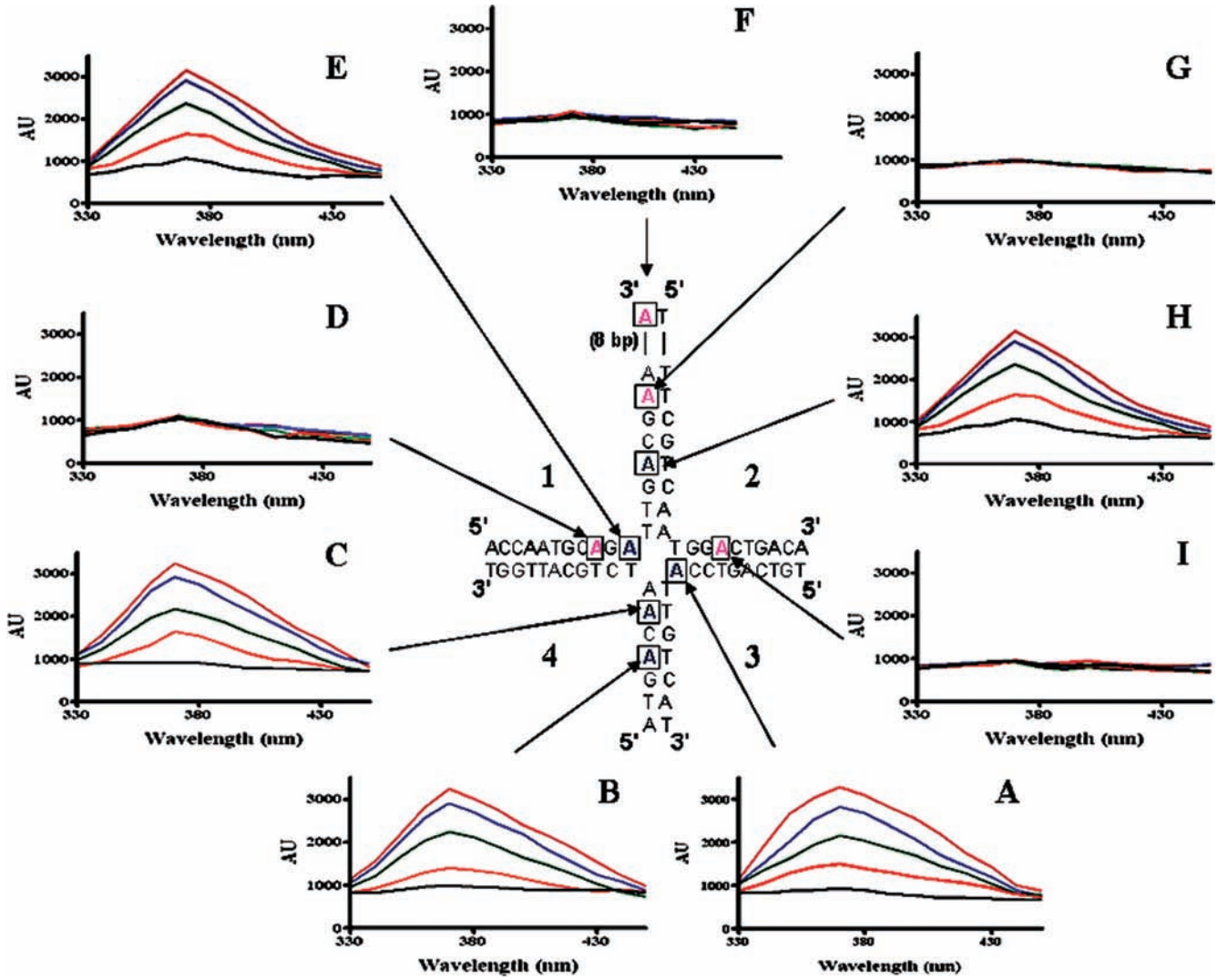

FIGURE 10: *M. tuberculosis* RuvA-induced structural distortion of homologous HJ as monitored using 2-AP fluorescence. The center panel shows the positions of the adenine bases (boxed), individually substituted with 2-AP, at the junction center and in the arms of the HJ. The corrected fluorescence emission spectra were recorded, in the wavelength region between 330 and 450 nm, as a function of increasing concentration of MtRuvA. In each reaction, 100 nM junction DNA was used. (A−I) Plots of the change in fluorescence intensity (in arbitrary units), on the *Y*-axis, in the absence (black lines) or presence of MtRuvA at 0.5 μM (red lines), 1 μM (green lines), 2.5 μM (blue lines), or 5 μM (purple lines). The fluorescence emission spectrum of each HJ variant is pointed with a black arrow to its corresponding 2-AP residue in the HJ diagram depicted at the center.

(Figure 11B, lanes 1−6). On the other hand, all the HJ variants complexed with MtRuvA exhibited retarded mobility. Interestingly, two HJ variants bound by MtRuvA exhibited relatively faster migration in the presence of both EDTA and Mg^{2+} (compare panels A and B of Figure 11, lanes 8 and 11). In slow-migrating complexes, the angle between long arms is 90°, whereas in fast-migrating complexes, the long arms are colinear. The control reaction in mixtures treated with proteinase K or SDS abolished the ability of MtRuvA to change the global conformation of HJs (data not shown).

DISCUSSION

In this study, we have examined the function of MtRuvA both in vivo and in vitro. To characterize its activity in vivo, we performed genetic complementation using *E. coli* Δ*ruvA* mutants for survival to genotoxic stress caused by different DNA-damaging agents. Despite the fact that the amino acid sequence of MtRuvA is only 33% identical with that of *E. coli* RuvA, the data presented here suggest that MtRuvA may form a functional complex with *E. coli* RuvB and RuvC (or works sequentially with *E. coli* RuvB and RuvC) in vivo to complement the defects of Δ*ruvA* mutants. In contrast, *Mycoplasma pneumoniae* RuvA was unable to complement *E. coli ruvA* mutants in DNA repair (*55*). In vitro studies suggest that *E. coli* RuvA and RuvB proteins together catalyze branch migration of Holliday junctions in an ATP-dependent manner; however, the intrinsic properties of RuvA and the underlying molecular mechanism remain poorly understood. Using synthetic Holliday junctions bearing either homologous or heterologous arms, we provide strong evidence that MtRuvA alone can induce structural distortions in the Holliday junctions. More importantly, our data disclose that MtRuvA causes two distinct, equally important, structural distortions between the homologous and heterologous Holliday junctions. The biological significance of the two modes of structural distortion by MtRuvA and the

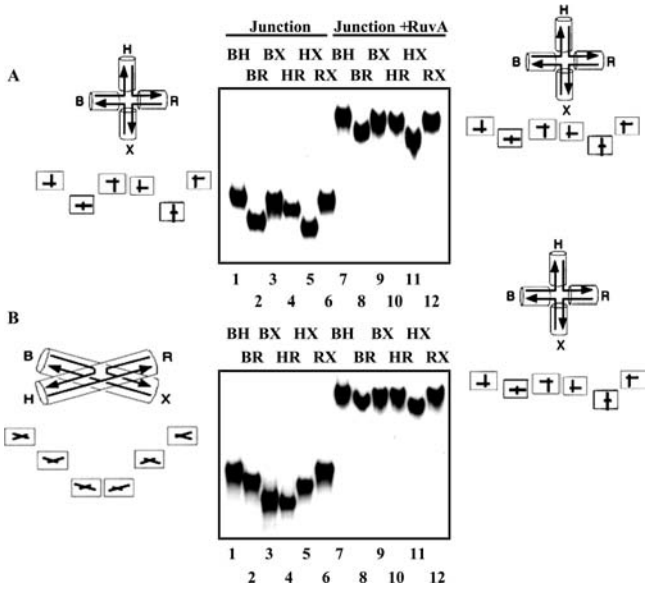

FIGURE 11: *M. tuberculosis* RuvA alters the global conformation of the Holliday junction. (A) Conformation of RuvA−HJ complexes in the presence of EDTA (lanes 1−6). Interpretation of these junctions is given on the left-hand side of the figure. MtRuvA−junction complexes (lanes 7−12) migrate as discrete bands, retarded with respect to the free junction DNA, but there is no change in the global conformation as the 4:1 mobility pattern is retained. An interpretation of the conformation of DNA within the complex is shown at the right. (B) Conformation of the MtRuvA−HJ complex in the presence of $MgCl_2$. In the presence of 100 μM $MgCl_2$, the HJ variants exhibit the characteristic "smile" arrangement (lanes 1−6) during polyacrylamide gel electrophoresis. Under the conditions described for panel A (lanes 7−12), all the junction variants bound to MtRuvA exhibited a similar mobility as seen in the presence of EDTA. An interpretation of the conformation of MtRuvA−HJ complexes is shown at the right.

implications for its role in recombinational repair and HR are discussed below.

In *E. coli*, RuvA, RuvB, and RuvC proteins process the branched DNA intermediates generated during the late stages of recombinational repair and HR (*56*). These results are consistent with *ruvA*, *ruvB*, or *ruvC* mutant phenotypes which are characterized by increased sensitivity to UV light, ionizing radiation, mitomycin C, and reduction in the efficiency of recombination under certain genetic backgrounds (*32*, *57*, *58*). Structural, biochemical, and mutational analyses indicate that *E. coli* RuvA is a Holliday junction-specific DNA binding protein, which then recruits RuvB to the HJ, leading to the formation of a tripartite protein complex. In this complex, the RuvA tetramer is flanked by two RuvB hexameric rings on opposite sides. Interestingly, RuvA forms two types of protein−HJ complexes: complex I, in which a single tetramer bound to the open conformation of the junction, and complex II, in which the octameric RuvA sandwiches the same junction. Binding of RuvA to the Holliday junction results in the isomerization of the junction from the stacked folded conformation to a square-planar structure in which all four arms are related by 90°. The binding of a dimeric RuvC, a structure-specific endonuclease, culminates in the formation of the RuvABC protein complex, which catalyzes the resolution of the junction (*59*).

The crystal structure of octameric MtRuvA has been determined at the atomic level (*41*). The cocrystal structure of the *M. leprae* octameric RuvA−HJ complex contains two tetramers bound to both sides of the junction (*17*). Neutron scattering studies have shown the existence of an octameric *M. leprae* RuvA−HJ complex in solution (*60*). Indeed, ultracentrifugation analysis corroborated the existence of a dynamic equilibrium between tetramers and octamers of *M. leprae* RuvA in solution, suggesting that a similar equilibrium between complexes I and II is most probable (*60*). The structures of *E. coli* RuvA−HJ complex I showed that the junction did not have a strictly square-planar conformation as the crossover point deviated closer to the concave surface of the RuvA tetramer. In contrast, the junction in complex II obtained with RuvA from *M. leprae* had a planar conformation. In the complex of the tetramer of *E. coli* RuvA with HJ, the two base pairs embedded symmetrically at the crossover point were disrupted, whereas in the octamer of the *M. leprae* RuvA−HJ complex, the DNA structure was found to be disordered and the junction conformation was not described in detail (*18*, *19*). Thus, the crystal structures of RuvA−HJ complexes not only provided an atomic view of the specific recognition between RuvA and the HJ but also revealed a probable role for RuvA in base pair rearrangements.

The paucity of extensive studies examining the biochemical properties of each member of the RuvABC protein complex restricts models in deciphering the functions of the individual components of the tripartite protein complex and their interactions to a speculative nature. Therefore, our goal is to gain mechanistic insights into the functions of the RuvABC protein complex, its subcomplexes, and individual subunits and integrate this information into the overall mechanistic pathway of HR in mycobacteria. Proteins that participate in HR of *M. tuberculosis* are more challenging to characterize than the prototype proteins from *E. coli* due to the lack of suitable genetic tools for analysis of their function in vivo. To this end, we performed detailed investigations, including genetic analysis, DNA binding, and Holliday junction distortion activities of MtRuvA. The gel mobility shift assays showed that MtRuvA binds HJ, in preference to any other DNA substrate. In contrast, *Mycoplasma pneumoniae* RuvA binds with high affinity to the Holliday junction, it also exhibits increased affinity for Y-shaped and duplex DNA substrates (*55*). As with *E. coli* RuvA and *M. leprae* RuvA, we found a striking correlation in the formation of two discrete complexes with progressively slower mobility as the concentration of RuvA used was increased. In agreement with *E. coli* RuvA, MtRuvA formed a faster-migrating complex I and slower migrating complex II with HJ, but not with other DNA substrates. However, sufficient data for fully understanding the functional roles of the two complexes are not available. The complex formed by RuvA with HJ was very stable. In the presence of Mg^{2+}, the Holliday junctions are folded into a stacked X conformation but adopt an unfolded square-planar structure in the absence of added metal ions (*61*). Consistent with some junction-binding proteins (*62*), MtRuvA binds the Holliday junction and maintains its global structure in an extended, unstacked conformation in a manner that was independent of the presence of Mg^{2+}. The conformation of the HJ deduced by comparative gel electrophoresis of RuvA approximates a tetrahedral arrangement of the junction arms, which is believed to facilitate branch migration.

As mentioned earlier, previous mechanistic and structural studies on RuvA have been performed with heterologous Holliday junction substrates. This leaves unanswered several

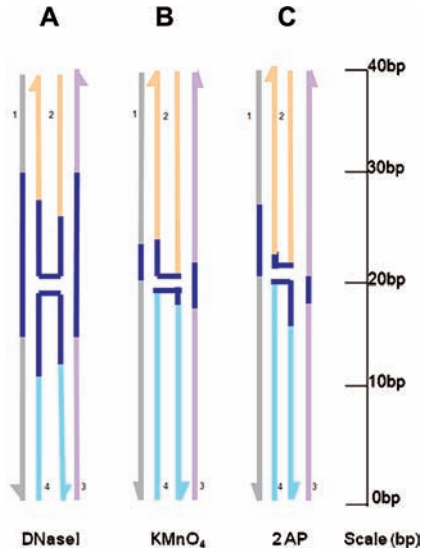

FIGURE 12: Schematic of the MtRuvA footprint on HJ as inferred from protection from DNase I cleavage (A), $KMnO_4$ probing (B), and 2-AP fluorescence emission (C). The region of protection or distortion on all strands of the HJ is colored blue over color-coded strands. For details, see the text.

questions about how RuvA functions in different contexts. For instance, how does RuvA act, in the absence of RuvB, when it encounters homologous HJ arms that are found in the cell during HR? Our studies tested this hypothesis, and the foregoing results provide direct experimental support for the notion that RuvA-induced distortion in the HJ is context-dependent. DNase I, chemical footprinting, and 2-AP fluorescence measurements suggest that binding of MtRuvA to the heterologous or homologous Holliday junction is asymmetric. Similar analysis of the *E. coli* RuvA−Holliday junction complex indicated symmetric binding covering 9−10 bp on all four arms of the HJ (reviewed in refs *4* and *5*). Figure 12 shows a composite view of the footprint generated by MtRuvA on HJ as inferred from DNase I protection, 2-AP fluorescence emission, and reactivity of bases to $KMnO_4$. The robust binding of MtRuvA to the junction center provides a mechanistic basis for it to facilitate branch migration. These results are in excellent agreement with the crystal structures of the *E. coli* RuvA−Holliday junction complex which show that the tetramer of RuvA extends over eight bases of the crossover point of the Holliday junction (*19*). Further experiments were performed to analyze MtRuvA−Holliday junction complexes using a sensitive fluorescence spectroscopic approach. Equilibrium 2-AP fluorescence measurements offered an independent method of unambiguously demonstrating structural distortion in HJ caused by MtRuvA. Consistent with previous crystallographic evidence with the *E. coli* RuvA−HJ complex (*19*), binding of MtRuvA to the heterologous HJ caused disruption of two base pairs located symmetrically at the crossover point. Significantly, on the other hand, MtRuvA was able to cause more extensive disruption along homologous HJ arms. Since RuvA is not an ATPase, we believe that the driving force behind the limited structural distortion of HJ is provided by RuvA binding to the HJ. The fact that two diverse approaches yielded such similar results is strong evidence that MtRuvA does indeed induce structural distortion of the arms in the homologous HJ. Our results underline the possible existence of distinct pathways for RuvA function, which presumably depend on the structure and the nature of the DNA repair or HR intermediates. Why does MtRuvA not disrupt base pairing in the arms of the heterologous HJ? How does MtRuvA distinguish between homologous and heterologous Holliday junctions? Additional experiments are necessary to gain insights into these issues and into the precise role of RuvA in RuvB-catalyzed branch migration.

In summary, our investigations show that binding of MtRuvA to the HJ induced changes in the local conformation of the junction, which might augment RuvB-catalyzed branch migration. An unexpected finding is the observation that MtRuvA causes two distinct types of structural distortions, depending on whether the Holliday junction contains homologous or heterologous arms. To the best of our knowledge, this is the first quantitative assessment and direct evidence in support of distinct structural distortions of homologous and heterologous HJ arms caused by any known Holliday junction binding protein.

REFERENCES

1. Bianco, P. R., Tracy, R. B., and Kowalczykowski, S. C. (1998) DNA strand exchange proteins: A biochemical and physical comparison. *Front. Biosci. 3*, D570−D603.
2. Lusetti, S. L., and Cox, M. M. (2002) The bacterial RecA protein and the recombinational DNA repair of stalled replication forks. *Annu. Rev. Biochem. 71*, 71–100.
3. West, S. C. (2003) Molecular views of recombination proteins and their control. *Nat. Rev. Mol. Cell Biol. 4*, 435–445.
4. West, S. C. (1997) Processing of recombination intermediates by the RuvABC proteins. *Annu. Rev. Genet. 31*, 213–244.
5. McGlynn, P., and Lloyd, R. G. (2002) Recombinational repair and restart of damaged replication forks. *Nat. Rev. Mol. Cell Biol. 3*, 859–870.
6. Yamada, K., Ariyoshi, M., and Morikawa, K. (2004) Three-dimensional structural views of branch migration and resolution in DNA homologous recombination. *Curr. Opin. Struct. Biol. 14*, 130–137.
7. Kuzminov, A. (1999) Recombinational repair of DNA damage in *Escherichia coli* and bacteriophage lambda. *Microbiol. Mol. Biol. Rev. 63*, 751–813.
8. Hiom, K., Tsaneva, I. R., and West, S. C. (1996) The directionality of RuvAB-mediated branch migration: *In vitro* studies with three-armed junctions. *Genes Cells 1*, 443–451.
9. McGlynn, P., and Lloyd, R. G. (2001) Action of RuvAB at replication fork structures. *J. Biol. Chem. 276*, 41938–41944.
10. Baharoglu, Z., Petranovic, M., Flores, M., and Michel, B. (2006) RuvAB is essential for replication forks reversal in certain replication mutants. *EMBO J. 25*, 596–604.
11. Michel, B., Boubakri, H., Baharoglu, Z., LeMasson, M., and Lestini, R. (2007) Recombination proteins and rescue of arrested replication forks. *DNA Repair 6*, 967–980.
12. Baharoglu, Z., Bradley, A. S., LeMasson, M., Tsaneva, I., and Michel, B. (2008) *ruvA* mutants that resolve Holliday junctions but do not reverse replication forks. *PLoS Genet. 4*, e1000012.
13. Donaldson, J. R., Courcelle, C. T., and Courcelle, J. (2004) RuvAB and RecG are not essential for the recovery of DNA synthesis following UV-Induced DNA damage in *Escherichia coli*. *Genetics 166*, 1631–1640.
14. Donaldson, J. R., Courcelle, C. T., and Courcelle, J. (2006) RuvABC is required to resolve Holliday junctions that accumulate following replication on damaged templates in *Escherichia coli*. *J. Biol. Chem. 281*, 28811–28821.
15. Iwasaki, H., Takahagi, M., Nakata, A., and Shinagawa, H. (1992) *Escherichia coli* RuvA and RuvB proteins specifically interact with Holliday junctions and promote branch-migration. *Genes Dev. 6*, 2214–2220.
16. Tsaneva, I. R., Müller, B., and West, S. C. (1992) ATP-dependent branch-migration of Holliday junctions promoted by the RuvA and RuvB proteins of *E. coli*. *Cell 69*, 1171–1180.
17. Chamberlain, D., Keeley, A., Aslam, M., ArenasLicea, J., Brown, T., Tsaneva, I. R., and Perkins, S. J. (1998) A synthetic Holliday junction is sandwiched between two tetrameric *Mycobacterium leprae* RuvA structures in solution: New insights from neutron scattering contrast variation and modeling. *J. Mol. Biol. 284*, 385–400.

18. Roe, S. M., Barlow, T., Brown, T., Oram, M., Keeley, A., Tsaneva, I. R., and Pearl, L. H. (1998) Crystal structure of an octameric RuvA-Holliday junction complex. *Mol. Cell 2*, 361–372.
19. Ariyoshi, M., Nishino, T., Iwasaki, H., Shinagawa, H., and Morikawa, K. (2000) Crystal structure of the Holliday junction DNA in complex with a single RuvA tetramer. *Proc. Natl. Acad. Sci. U.S.A. 97*, 8257–8262.
20. Hargreaves, D., Rice, D. W., Sedelnikova, S. E., Artymiuk, P. J., Lloyd, R. G., and Rafferty, J. B. (1998) Crystal structure of *E. coli* RuvA with bound DNA Holliday junction at 6 Å resolution. *Nat. Struct. Biol. 5*, 441–446.
21. Iwasaki, H., Takahagi, M., Shiba, T., Nakata, A., and Shinagawa, H. (1991) *Escherichia coli* RuvC protein is an endonuclease that resolves the Holliday structure. *EMBO J. 10*, 4381–4389.
22. Dunderdale, H. J., Benson, F. E., Parsons, C. A., Sharples, G. J., Lloyd, R. G., and West, S. C. (1991) Formation and resolution of recombination intermediates by *E. coli* RecA and RuvC proteins. *Nature 354*, 506–510.
23. Lloyd, R. G., Benson, F. E., and Shurvinton, C. E. (1984) Effect of *ruv* mutations on recombination and DNA repair in *Escherichia coli K-12*. *Mol. Gen. Genet. 194*, 303–309.
24. Davies, A. A., and West, S. C. (1998) Formation of RuvABC-Holliday junction complexes *in vitro*. *Curr. Biol. 8*, 725–727.
25. van Gool, A. J., Hajibagheri, N. M., Stasiak, A., and West, S. C. (1999) Assembly of the *Escherichia coli* RuvABC resolvasome directs the orientation of Holliday junction resolution. *Genes Dev. 13*, 1861–1870.
26. Zerbib, D., Mezard, C., George, H., and West, S. C. (1998) Coordinated actions of RuvABC in Holliday junction processing. *J. Mol. Biol. 281*, 621–630.
27. Muniyappa, K., Vaze, M. B., Ganesh, N., Sreedhar Reddy, M., Guhan, N., and Venkatesh, R. (2000) Comparative genomics of *Mycobacterium tuberculosis* and *Escherichia coli* for recombination (rec) genes. *Microbiology 146*, 2093–2095.
28. Vaze, M. B., and Muniyappa, K. (1999) RecA protein of *Mycobacterium tuberculosis* possesses pH-dependent homologous DNA pairing and strand exchange activities: Implications for allele exchange in *mycobacteria*. *Biochemistry 38*, 3175–3186.
29. Muniyappa, K., Ganesh, N., Guhan, N., Singh, P., Manjunath, G. P., Datta, S., Chandra, N. R., and Vijayan, M. (2004) Homologous recombination in *mycobacteria*. *Curr. Sci. 86*, 141–148.
30. Ganesh, N., and Muniyappa, K. (2003) Characterization of DNA strand transfer promoted by *Mycobacterium smegmatis* RecA reveals functional diversity with *Mycobacterium tuberculosis* RecA. *Biochemistry 42*, 7216–7225.
31. Venkatesh, R., Ganesh, N., Guhan, N., Reddy, M. S., Chandrasekhar, T., and Muniyappa, K. (2002) RecX protein abrogates ATP hydrolysis and strand exchange promoted by RecA: Insights into negative regulation of homologous recombination. *Proc. Natl. Acad. Sci. U.S.A. 99*, 12091–12096.
32. Hishida, T., Iwasaki, H., Ishioka, K., and Shinagawa, H. (1996) Molecular analysis of *Pseudomonas aeruginosa* genes, *ruvA*, *ruvB* and *ruvC*, involved in processing of homologous recombination intermediates. *Gene 182*, 63–70.
33. Sambrook, J., Fritsch, E. F., and Maniatis, T. (1989) *Molecular Cloning: A Laboratory Manual*, 2nd ed., Cold Spring Harbor Laboratory Press, Plainview, NY.
34. Ausubel, F. M., Brent, R., Kingston, R. E., Moore, D. D., Seidman, J. G., Smith, J. A., and Struhl, K. (1987) *Current Protocols in Molecular Biology*, Greene Publishing Associates and Wiley-Interscience, John Wiley & Sons, New York.
35. Maxam, A. M., and Gilbert, W. (1980) Sequencing end labeled DNA with base-specific chemical cleavages. *Methods Enzymol. 65*, 499–560.
36. Dèclais, A.-C., and Lilley, D. M. J. (2000) Extensive central disruption of a four-way junction on binding CCE1 resolving enzyme. *J. Mol. Biol. 296*, 421–433.
37. Sanchez, H., Kidane, D., Reed, P., Curtis, F. A., Cozar, M. C., Graumann, P. L., Sharples, G. J., and Alonso, J. C. (2005) The RuvAB branch migration translocase and RecU Holliday junction resolvase are required for double-stranded DNA break repair in *Bacillus subtilis*. *Genetics 171*, 873–883.
38. Parsons, C. A., Kemper, B., and West, S. C. (1990) Interaction of a four-way junction in DNA with T4 endonuclease VII. *J. Biol. Chem. 265*, 9285–9289.
39. Parsons, C. A., Tsaneva, I., Lloyd, R. G., and West, S. C. (1992) Interaction of *Escherichia coli* RuvA and RuvB proteins with synthetic Holliday junctions. *Proc. Natl. Acad. Sci. U.S.A. 89*, 5452–5456.
40. Arenas-Licea, J., van Gool, A. J., Keeley, A. J., Davies, A., West, S. C., and Tsaneva, I. R. (2000) Functional Interactions of *Mycobacterium leprae* RuvA with *Escherichia coli* RuvB and RuvC on Holliday Junctions. *J. Mol. Biol. 301*, 839–850.
41. Rajan Prabu, J., Thamotharan, S., Khanduja, J. S., Alipio, E. Z., Kim, C., Waldo, G. S., Terwilliger, T. C., Segelke, B., Lekin, T., Toppani, D., Hung, L., Yu, M., Bursey, E., Muniyappa, K., Chandra, N. R., and Vijayan, M. (2006) Structure of *Mycobacterium tuberculosis* RuvA, a protein involved in recombination. *Acta Crystallogr. F62*, 731–734.
42. Duckett, D. R., Murchie, A. I., Diekmann, S., von Kitzing, E., Kemper, B., and Lilley, D. M. (1988) The structure of the Holliday junction and its resolution. *Cell 55*, 79–89.
43. Iida, S., and Hayatsu, H. (1971) The permanganate oxidation of thymidine and thymidylic acid. *Biochim. Biophys. Acta 228*, 1–8.
44. Sasse-Dwight, S., and Gralla, J. D. (1991) Footprinting protein-DNA complexes *in vivo*. *Methods Enzymol. 206*, 146–168.
45. Murchie, A. I. H., Carter, W. A., Portugal, J., and Lilley, D. M. J. (1990) The tertiary structure of the four-way DNA junction affords protection against DNase I cleavage. *Nucleic Acids Res. 18*, 2599–2606.
46. Hiom, K., and West, S. C. (1995) Branch migration during homologous recombination: Assembly of a RuvAB-Holliday junction complex *in vitro*. *Cell 80*, 787–793.
47. Seigneur, M., Bidnenko, V., Ehrlich, S. D., and Michel, B. (1998) RuvAB acts at arrested replication forks. *Cell 95*, 419–430.
48. Privezentzev, C. V., Keeley, A., Sigala, B., and Tsaneva, I. R. (2005) The role of RuvA octamerization for RuvAB function *in vitro* and *in vivo*. *J. Biol. Chem. 280*, 3365–3375.
49. Whitby, M. C., Bolt, E. L., Chan, S. N., and Llyod, R. G. (1996) Interactions between RuvA and RuvC at Holliday junctions: Inhibition of junction cleavage and formation of a RuvA-RuvC-DNA complex. *J. Mol. Biol. 264*, 878–890.
50. Parsons, C. A., Stasiak, A., Bennett, R. J., and West, S. C. (1995) Structure of a multisubunit complex that promotes DNA branch-migration. *Nature 374*, 375–378.
51. White, M. F., and Lilley, D. M. J. (1997) The resolving enzyme CCE1 of yeast opens the structure of the four-way DNA junction. *J. Mol. Biol. 266*, 122–134.
52. Giraud-Panis, M.-J. E., and Lilley, D. M. J. (1998) Structural recognition and distortion by the DNA junction resolving enzyme RusA. *J. Mol. Biol. 278*, 117–133.
53. Gough, G. W., and Lilley, D. M. J. (1985) DNA bending induced by cruciform formation. *Nature 313*, 154–156.
54. Cooper, J. P., and Hagerman, P. J. (1987) Gel electrophoretic analysis of the geometry of a DNA four-way junction. *J. Mol. Biol. 198*, 711–719.
55. Ingleston, S. M., Dickman, M. J., Grasby, J. A., Hornby, D. P., Sharples, G. J., and Lloyd, R. G. (2002) Holliday junction binding and processing by the RuvA protein of *Mycoplasma pneumoniae*. *Eur. J. Biochem. 269*, 1525–1533.
56. Benson, F. E., Collier, S., and Lloyd, R. G. (1991) Evidence of abortive recombination in *ruv* mutants of *Escherichia coli K-12*. *Mol. Gen. Genet. 225*, 266–272.
57. Sharples, G. J., Benson, F. E., Illing, G. T., and Lloyd, R. G. (1990) Molecular and functional analysis of the *ruv* region of *Escherichia coli K-12* reveals three genes involved in DNA repair and recombination. *Mol. Gen. Genet. 221*, 219–226.
58. Luisi-DeLuca, C., Lovett, S. T., and Kolodner, R. D. (1989) Genetic and physical analysis of plasmid recombination in *recB recC sbcB* and *recB recC sbcA Escherichia coli K-12* mutants. *Genetics 122*, 269–278.
59. Eggleston, A. K., Mitchell, A. H., and West, S. C. (1997) In vitro reconstitution of the late steps of genetic recombination in *E. coli*. *Cell 89*, 607–617.
60. Lee, Y. C., Flora, R., McCafferty, J. A., Gor, J., Tsaneva, I. R., and Perkins, S. J. (2003) A tetramer-octamer equilibrium in *Mycobacterium leprae* and *Escherichia coli* RuvA by analytical ultracentrifugation. *J. Mol. Biol. 333*, 677–682.
61. Duckett, D. R., Murchie, A. I. H., and Lilley, D. M. J. (1990) The role of metal ions in the conformation of the four-way DNA junction. *EMBO J. 9*, 583–590.
62. Dèclais, A.-C., and Lilley, D. M. J. (2008) New insight into the recognition of branched DNA structure by junction-resolving enzymes. *Curr. Opin. Struct. Biol. 18*, 86–95.

BI8016526